Characteristics of gravity waves in the upper mesosphere region observed by OH airglow imaging

R. Sikha Pragati[1], Navin Parihar[2], Rupesh Ghodpage[2] and G. K. Mukherjee[3,*]

[1]Department of Physics, Andhra University, Visakhapatnam 500 003, India
[2]Dr K.S.K.G.R. Laboratory, IIG, Allahabad 221 505, India
[3]Indian Institute of Geomagnetism, Panvel (W), Navi Mumbai 410 218, India

We present the characteristics of small-scale (<100 km) gravity waves in the upper mesosphere region derived from OH airglow imaging observations at Allahabad (25.4°N, 81.8°E, dip lat. ~16.34°N) in India during January–May 2008 on cloud free and moonless nights. Horizontal and vertical propagation characteristics of the short period (<1 h) gravity waves (wavelength, apparent phase velocity, periodicity, direction) have been retrieved. Observed period, horizontal wavelength and observed horizontal phase speeds of gravity waves were typically 5–17 min, 10–37 km and 10–48 m/s. The propagation directions are in north and north-eastward in April and May. In February and March, few displays showed significant south-west motion. The possible source of wave generation has been discussed.

Keywords: Airglow, gravity waves, mesosphere, troposphere, thunderstorm.

ALL-SKY imaging of the airglow provides a unique record of the occurrence and propagation direction of atmospheric waves and other parameters. Gravity waves are important for understanding the energy and momentum flow in the MLT (mesosphere and lower thermosphere) region (80–100 km) of earth, where they can release momentum having propagated upwards from their respective generation regions in the troposphere and stratosphere. Wave dissipation affects wind and temperature in the upper MLT. These waves have been studied by airglow imaging techniques, radar, imaging riometers and lidar[1–12]. Majority of the waves arise in the lower atmosphere by weather related disturbances such as convection activity, storms, fronts, squall lines, jet streams and due to orographic origin (wind blowing over mountains) and other processes.

Observations reveal that gravity waves range with horizontal wavelengths in the range ~5–500 km, vertical wavelengths ~0.1–50 km, and oscillation periods between about 5 min and a day[4]. Using image data of OH emissions from Shigaraki (35°N, 136°E), Nakamura *et al.*[13] found a seasonal variation of wave parameters. For the gravity waves with horizontal wavelength longer than 18 km, the propagation direction was eastward in summer and westward in winter. Medeiros *et al.*[14] observed that the propagation direction of gravity waves were towards south-east in summer and north-west in winter at Cachoeira Paulista (CP; 23°S, 45°W) in Brazil. Although the main characteristics of these waves seem to be understood, their detailed behaviour with geographic and geomagnetic location have not been studied well.

In this article, we describe the new imaging observations of short-period gravity waves observed from a low latitude station, Allahabad during January–May 2008. These are the first imaging observations of gravity waves from this latitude region in India. The data give vital information about apparent horizontal phase velocity, direction, wavelength and period of these waves. This collective data along with geographical locations, shape, orientation and time of displays have been very helpful in investigating the main sources of these waves.

Principle of OH emission

The Meinel band hydroxyl emits radiation so that the excited hydroxyl radicals (OH*) immediately transfer to the lower stable energy level. OH* is considered to be produced by the following reactions.

$$O_3 + H \rightarrow OH^* (\nu \leq 9) + O_2,$$

$$HO_2 + O \rightarrow OH^* (\nu \leq 6) + O_2,$$

$$O_2^* + H \rightarrow O + OH^*,$$

$$OH^*(\nu) \rightarrow OH^{**}(\nu') + h\nu\,(550\ \text{nm}-4.4\ \mu\text{m}),$$

where * and ** indicate that the molecule is in a state of excitation, and ν and ν' indicate the order of states of molecules. The peak altitudes of the OH emission layers were observed to be ~87 km respectively, with a layer width of ~11 km each[15]. These emissions exhibit considerable spatial and temporal fluctuations that have been

*For correspondence. (e-mail: gkm@iigs.iigm.res.in)

attributed to the passage of atmospheric gravity waves through the airglow layers.

The all-sky imaging system

The all-sky imaging system used in the present study consists of three parts: an optical system, a detector and an operating note book PC (hp).

A schematic diagram for the optical layout of the all-sky imager is presented in Figure 1. The optical system collects light from 180° field of view with a Mamiya RB fish eye lens that has focal length of 24 mm and focal ratio of 4. The collected light beam is collimated by a telecentric optical plano-convex lens combination to pass through a narrow-band filter with nearly perpendicular to incidence angles. Six filters can be used among six filter positions of a filter drum. The OH broad-band filter (720–910 nm) used here has 87% transparency and blocking between 850 and 870 nm with a notch at 868 nm to avoid O_2 (0, 1) atmospheric bands. The collimated beam after the filter (~69 mm diameter) is fed to a Canon camera lens (50 mm, f/0.95) mounted on to the CCD camera to make an image on to the CCD detector's active image area. The detector is a thermoelectrically cooled CCD camera (PIXIS 512) kept at a temperature of –70° to reduce the thermal noise. The CCD chip has 512×512 square pixels of 24 microns. The filter wheel and camera shutter are controlled by a notebook PC (hp) with an operating system, Windows XP through WINVIEW software.

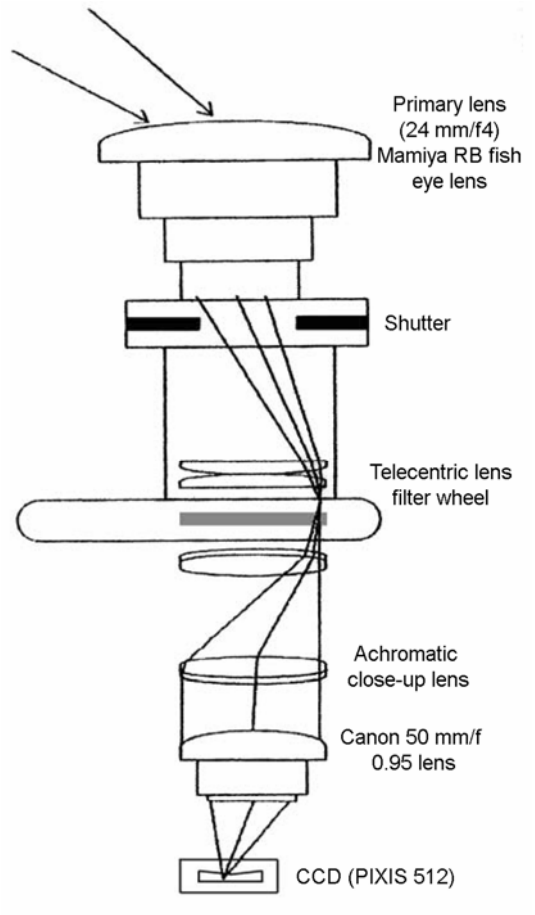

Figure 1. Schematic of the optical ray paths of the all-sky imager.

Observations of OH airglow and gravity wave characteristics

The wide-angle imaging technique offers the unique capability to characterize simultaneously the propagation of gravity wave phenomena over a large geographical region. For the present study, we have used the OH airglow images collected between January and May at a tropical station, Dr K.S.K.G.R. Laboratory, Allahabad (25.4°N, 81.8°E), on cloud free and moonless nights. These observations were carried out around the new moon period during 20:00 to 05:00 h (a total of 9 h) of succeeding day in consecutive months January, February, March, April and May 2008. The decimetric solar flux indices (F10.7 cm) for all the days of our observation varied between 67 and 85 (units of 10^{-22} W m^{-2}). The magnetic activity (Ap) indices ranged between 01 and 36.

In the present study, we define a gravity wave event as the occurrence of a sequence of airglow images showing coherent wave fronts propagating in a given direction with duration of more than 30 min for bands. In the beginning, the CCD images are processed by subtracting background images and then dividing them by suitable flat field images[10]. The nonuniformity of the image due to Van Rhijn effect, atmospheric extinction and nonuniform sensitivity of the imager at different pixels is roughly corrected by this process. The fish eye lens images are then transformed into an image in geographic coordinates by assuming an altitude (87 km) of the OH airglow emission layer. After processing the all-sky images, from a warped image to an unwarped one, the gravity wave parameters, horizontal wavelength, period, phase velocity and propagation direction are retrieved from successive images by knowing the size of the images transformed into the geographical coordinates and the time difference of two sequential images respectively. The imager field of view with 75° zenith angle is 500 km diameter at an altitude of 87 km.

Wave structure was detected at almost all azimuths up to a range of ~500 km (limited by the local horizon and assuming emission altitude of 87 km) on 22 occasions during this period, out of which only 16 nights of quality data featuring gravity wave phenomena observed were selected for the present study and the nightglow observations contaminated with clouds were discarded for the period of study. Out of these 16 events obtained, 14 were of the band-type origin and two days showed ripple-type structure (Figure 2). It is believed that the band type

waves have a phase propagating mode with a long distance (longer than a few hundred km) and transport momentum. They are different from the ripple type which could be generated locally by wind shearing and/or wave to wave interaction[16,17].

Figure 3 shows the signature of gravity waves in OH emissions on the night of 29 January 2008 at Allahabad. The structure showed a well-defined OH-pattern with near SE–NW aligned wavefronts extending over the whole field of view of the camera.

Table 1 lists the azimuth of the wave motions (i.e. the normal to the wavefronts) along with their date, timings, observed phase speeds and horizontal wavelengths for 14 displays recorded. On two occasions (27 March and 7 April), two wave patterns crossing each other in perpendicular directions were observed during the night. The gravity waves were observed between 20:00 and 03:00 h. Their horizontal phase speeds varied between 10 and 48 m/s and the wavelengths between 10 and 37 km. The azimuth of the wave motions was determined to an accuracy of about ± 5°. Overall, the gravity waves were observed in time less than an hour. It was usually easier to determine the orientation and direction of motion of the wave pattern than to accurately measure its speed of their movement. It showed a clear preference for wave propagation generally toward the north-east (in total 71% of the wave azimuths were within 45° NE). In February and March, few displays also exhibited significant south-west motion. In April, the north-east motion was even more prominent with no wave motion in the south-west direction.

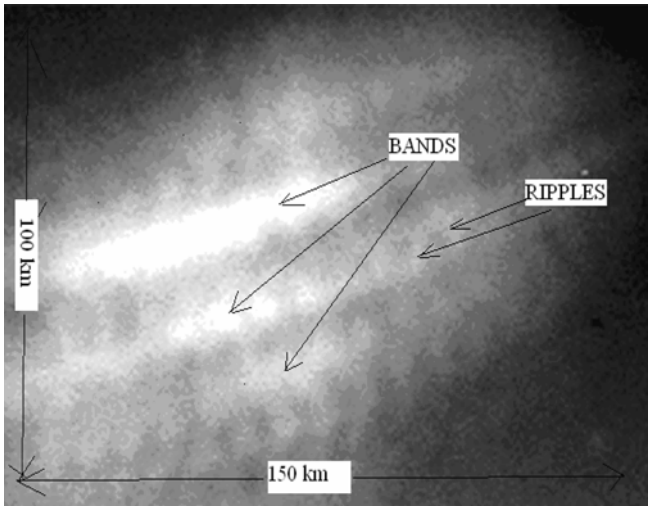

Figure 2. Gravity waves showing band and ripple structures observed in OH emission (87 km) on the night of 4 February 2008 at Allahabad.

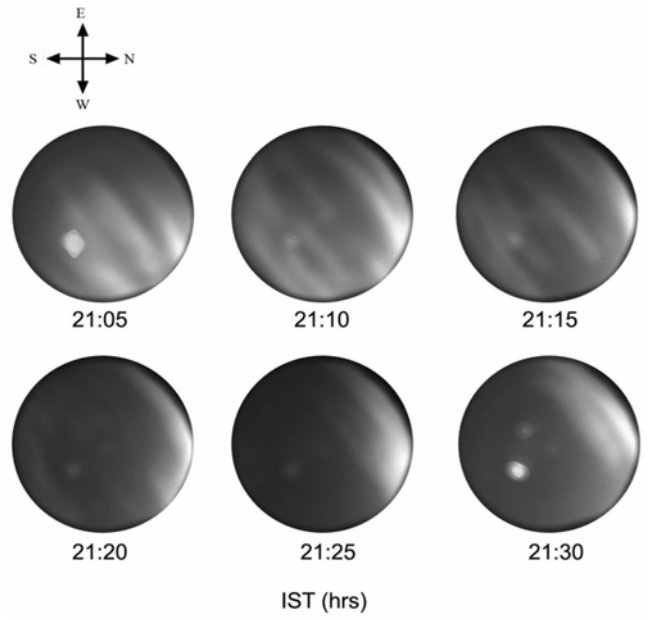

Figure 3. The signature of gravity waves observed in OH emission on the night of 29 January 2008 at Allahabad.

Figure 4 shows the histogram of the gravity wave phase speed, time periods and horizontal wavelength at Allahabad. The waves observed at Allahabad show apparent phase speed distributed between 10 and 48 m/s. The maximum occurrence is at 30–48 m/s. The waves observed at Allahabad show their time period between 5 and 19 min, the maximum occurrence takes place around 5–9 min. The horizontal wavelengths range between 10 and 37 km with maxima occurring at 10–19 km. Similar wave characteristics were also found at CP (22.7°N, 45°W) using an all-sky imager[18], the waves observed at CP show horizontal wavelength between 10 and 30 km with period between 6 and 16 min and horizontal phase speeds between 10 and 40 m/s. Using gravity wave data at CP, Taylor *et al.*[19] also observed the phase velocity varying between 10 and 45 m/s with a peak around 20–30 m/s.

Using a CCD-based all-sky imager, similar distributions of gravity waves were reported by Mukherjee[10] in hydroxyl OH and OI 557.7 nm images on the night of 18 February 2001 at Panhala (17°N, 74.2°E). The observed horizontal phase speeds (~50 m/s), wavelength (~25 km) and wave period (~8 min) of the gravity waves match with the findings of the present study.

Discussion and conclusions

Atmospheric gravity waves play an important role in the dynamics and energetics of the mesosphere, thermosphere and ionosphere. To understand these wave phenomena, we carried out imaging observations with CCD based all-sky imager at Allahabad on clear moonless nights during January–May 2008. The characteristics of horizontal propagation parameters (time period, apparent phase velocity and wavelength) of the gravity waves have been inferred from OH images (~87 km) observed at Allahabad. The results outlined are as follows.

Table 1. OH data analysis for February, March, April and May 2008

Date	Day number	Wave propagation time (h)	Wave azimuth	Observed phase speed (m/s)	Horizontal wavelength (km)
3 February 2008	34	00:10–00:52	260	43 ± 2	14
15 February 2008	46	01:21–02:16	30	22 ± 1	13
3 March 2008	63	00:06–01:19	45	10 ± 2	10
9 March 2008	69	21:50–22:25	220	18 ± 2	10
27 March 2008 (25)	87	20:00–20:48	260	36 ± 2	37
27 March 2008 (27)	87	21:26–22:41	300	35 ± 1	34
2 April 2008	93	20:34–21:55	10	37 ± 2	17
7 April 2008 (OH1)	98	20:33–22:54	45	40 ± 2	20
10 April 2008	101	01:51–02:31	40	12 ± 2	11
11 April 2008	101–102	23:24–00:04	30	31 ± 1	24
12 April 2008	103	00:40–01:56	15	28 ± 2	15
29 April 2008	120	01:09–02:31	45	36 ± 1	15
30 April 2008	121	02:49–03:08	40	48 ± 1	16
1 May 2008	122	20:05–21:45	20	40 ± 2	20

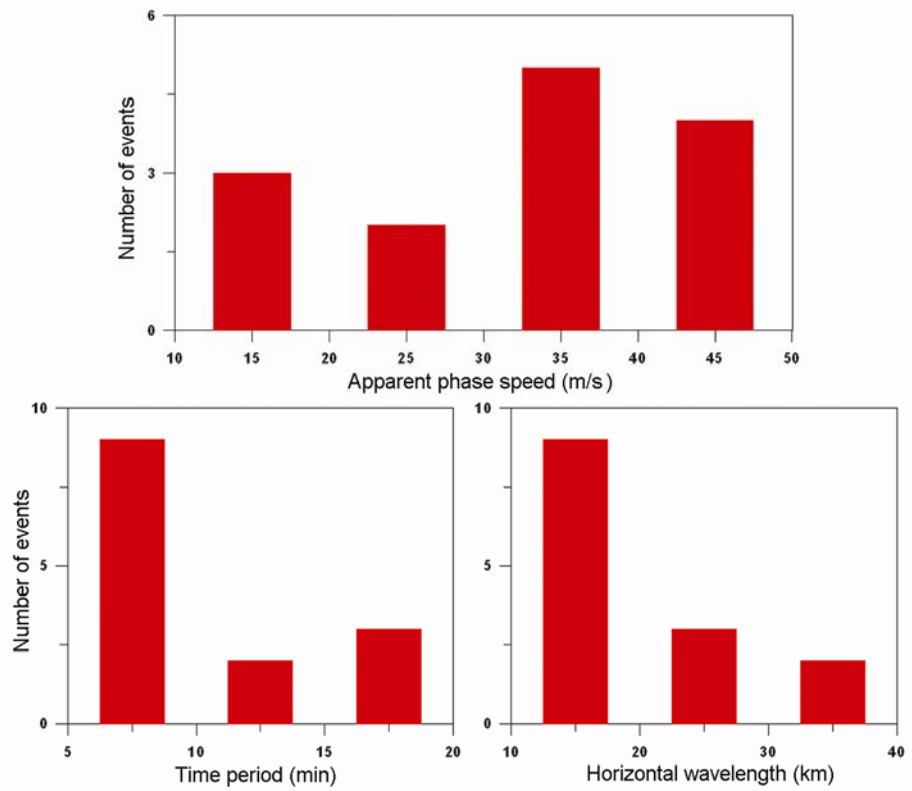

Figure 4. Frequency of occurrence of apparent phase speed (m/s), time period (min), horizontal wavelength (km) of the gravity waves.

Two types (band and ripple) of waves have been observed. The band type waves spread horizon–horizon in all-sky images. They are believed to be due to short period gravity waves that propagate free, horizontally and vertically[17]. The main feature of ripple type of waves is that their wave crests are aligned perpendicular to a band type of waves. The horizontal propagation direction of the gravity waves is an important parameter which indicates the direction of momentum transferred by such waves. The observed wave (band) propagation directions reveal that a major part of the waves has been directed towards north-east. Similar wave structures characterized by a horizontal wavelength of 5–37 km and phase velocity of 10–48 m/s are observed within the field of view of 75° zenith angle, indicating that the spatial extent of the short-period wave is more than 500 km. The spatial and temporal properties of the wave motions observed are typically of the low-latitude nightglow displays. On

occasions these displays have been observed with a time period of <19 min having horizontal phase velocity <49 m/s and horizontal wavelength less than 40 km.

In order to get the vertical propagation characteristics of gravity waves, the linear dispersion relation of the gravity wave is expressed as[20]:

$$m^2 = (N^2/(u - c)^2) - k^2 - 1/4H^2, \quad (1)$$

where m, N, u, c, k and H are the vertical wavenumber, Brunt–Väisälä frequency, background wind velocity, observed wave phase velocity, horizontal wavenumber and scale height respectively. The vertical (V_{gz}) and horizontal (V_{gx}) group velocity of the waves are derived from $V_{gz} = \partial\omega/\partial m$ and $V_{gx} = \partial\omega/\partial k$ (where the wave frequency, $\omega = ck$) to give[10]:

$$V_{gz} = \pm Nmk/(m^2 + k^2 + 1/4H^2)^{3/2}, \quad (2)$$

$$V_{gx} = u \pm N(m^2 + 1/4H^2)/(m^2 + k^2 + 1/4H^2)^{3/2}. \quad (3)$$

Equations (2) and (3) give the vertical and horizontal group velocities of wave energy propagation. It is seen that the vertical propagation of gravity waves is strongly influenced by horizontal wind velocity in the background.

We do not have the horizontal wind profile at the place of imaging observations, therefore, we have used HWM 93 model[21] to compute the values of the background wind velocity u. The values of c and k have been estimated from airglow measurements as shown in Table 1. In the atmosphere, the possible vertical propagation, $\omega^2 < N^2$. The realistic value of $N \sim 0.02$ rad/s has been assumed to compute the vertical wavelength and vertical group velocities. This corresponds to relaxation time $(2\pi/N) \sim 5$ min for the average atmosphere. The vertical wavelength, $L_v = 2\pi/m$, and the horizontal and vertical group velocities of the observed waves are computed using eqs (2) and (3) and are found to be varying between 10 km and 14 km, ±25–40 m/s and ±8–16 m/s. As the waves were observed over a very large area localized in the mesosphere, it is unlikely that the sources of the waves were localized. There is a possibility that if the source region is localized in the area but the wave is ducted in the MLT region and propagated horizontally, it is possible to have large horizontal extent.

The wave propagation direction in the mesopause region depends on two factors, its source location in the lower atmosphere relative to the observer, and the background wind field in the stratosphere and mesosphere. The preferential directions of wave propagation are mainly towards north and north-east in April and May at the observation site. This could be due to strong tropospheric convection in summer as has been suggested by several workers[22–24]. Some of the waves could be also produced due to Brunt–Doppler ducting[25] and/or waves generated *in situ* due to reflection at the mesopause. Nakamura *et al.*[23] reported that at low latitude MLT region, the propagation direction of short-period gravity waves was consistent with the spatial distribution of tropospheric clouds. These clouds mainly existed in the direction opposite to the propagation direction of gravity waves. Moreover, the equatorial middle atmosphere has weaker wind pattern and the Doppler shift to the atmospheric waves and associated wave filtering effect due to background neutral wind flow would be less significant.

There are many studies about gravity wave characteristics in the upper mesosphere region. One of the advantages of imaging technique is that horizontal propagation characteristics can be obtained in a more straightforward way than the radar measurements which rely on the theory of gravity waves[26]. Only some techniques can derive all the intrinsic wave parameters simultaneously. From the horizontal wave propagation characteristics and background wind information, also the vertical wavelength λ_z can be derived via the dispersion relation, but it does not provide the sense of vertical propagation. Radar and lidar techniques combined together can directly determine λ_z, including its sign (see, e.g. the radar results by Gavrilov *et al.*[27]), but are limited to $\lambda_z \leq 20$ km. The optical zenith observations as discussed by Reisin and Scheer[28] not only derive λ_z but also distinguish between upward and downward phase propagation. Due to some theories[18,26], the sign of the phase difference between gravity-wave induced brightness and rotational temperature oscillations of the same airglow emission depends directly on the sense of vertical propagation[28]. In future, with these gravity wave parameters both forward and reverse ray tracing methods[29] can be used to study the propagation characteristics of gravity waves through the middle atmosphere and the source region can be estimated.

1. Yang, G., Clemesha, B., Batista, P. and Dale, S., Lidar study of the characteristics of gravity waves in the mesopause region at a southern low-latitude location. *J. Atmos. Sol. Terr. Phys.*, 2008, **70**, 991–1011.
2. Moffat-Griffin, T., Hibbins, R. E., Nielsen, K., Jarvis, M. J. and Taylor, M. J., Observing mesospheric gravity waves with an imaging riometer. *J. Atmos. Sol. Terr. Phys.*, 2008, **70**, 1327–1335.
3. Taylor, M. J., Turnbull, D. N. and Lowe, R. P., Spectrometric and imaging measurements of a spectacular gravity wave event observed during the ALOHA-93 campaign. *Geophys. Res. Lett.*, 1995, **22**, 2849–2852.
4. Nakamura, T., Tsuda, T., Maekawa, R., Tsutsumi, T., Shiokawa, K. and Ogawa, T., Seasonal and variation of gravity waves with various temporal and horizontal scales in the MLT region observed with radar and airglow imaging. *Adv. Space Res.*, 2001, **27**, 1737–1742.
5. Swenson, G. R. and Liu, A. Z., A model for calculating of acoustic gravity wave energy and momentum flux in the mesosphere from OH airglow. *Geophys. Res. Lett.*, 1998, **25**, 477–480.
6. Tsuda, T. *et al.*, Coordinated observations of the mesopause region with radar and optical techniques. *Adv. Space Res.*, 2000, **26**, 907–916.
7. Ejiri, M. K., Shiokawa, K., Ogawa, T., Kubota, M., Nakamura, T. and Tsuda, T., Dual-site imaging observations of small-scale wave

structures through OH and OI nightglow emissions. *Geophys. Res. Lett.*, 2002, **29**, 1445–1448.
8. Shiokawa, K., Ejiri, M. K., Ogawa, T., Yamada, Y., Fukunishi, H., Igarashi, K. and Nakamura, T., A localized structure in OH airglow images near the mesopause region. *J. Geophys. Res.*, 2003, **108**, 4048–4053.
9. Liu, A. Z. and Swenson, G. R., A modeling study of O_2 and OH airglow perturbations induced by atmospheric gravity waves. *J. Geophys. Res*., 2003, **108**, 4151–4159.
10. Mukherjee, G. K., The signature of short period gravity waves imaged in OI 557.7 nm and near infrared OH nightglow emissions over Panhala. *J. Atmos. Sol. Terr. Phys*., 2003, **65**, 1329–1335.
11. Mukherjee, G. K., Optical observation of mesospheric gravity wave activity. International Conference on Trends in Optics and Photonics (ICON TOP 2009), 1–4 March 2009, pp. 331–338.
12. Laxmi Narayanan, V., Gurubaran, S. and Emperumal, K., Imaging observations of upper mesospheric nightglow emissions from Tirunelveli (8.7°N). *Indian J. Radio Space Phys*., 2009, **38**, 150–158.
13. Nakamura, T., Higashikawa, A., Tsuda, T. and Matsushita, Y., Seasonal variations of gravity wave structures in OH airglow with a CCD imager at Shigaraki. *Earth Planets Space,* 1999, **51**, 897–906.
14. Medeiros, A. F., Taylor, M. J., Takahashi, H., Batista, P. P. and Gobi, D., An investigation of gravity wave activity in the low-latitude upper mesosphere: propagation direction and wind filtering. *J. Geophys. Res.*, 2003, **108**, 4411–4419.
15. Mukherjee, G. K. and Parihar, N., Measurement of rotational temperature at Kolhapur, India. *Ann. Geophys.*, 2004, **22**, 3315–3321.
16. Taylor, M. J. and Hapgood, M. A., Identification of a thunderstorm as source of short period gravity waves in upper atmospheric night glow emission. *Planet Space Sci*., 1988, **36**, 975–985.
17. Taylor, M. J. and Hapgood, M. A., On the origin of ripple type wave structure in the nightglow emission. *Planet. Space Sci*., 1990, **38**, 1421–1430.
18. Hines, C. O., and Tarasick, D. W., On the detection and utilization of gravity waves in airglow studies. *Planet. Space Sci.*, 1987, **35**, 851–866.
19. Taylor, M. J., Pendleton Jr, W. R., Clark, S., Takahashi, H., Gobbi, D. and Goldberg, R. A., Image measurements of short-period gravity waves at equatorial latitudes. *J. Geophys. Res.*, 1997, **102**, 26283–26299.
20. Hines, C. O., Internal atmospheric gravity waves at ionospheric height. *Can. J. Phys*., 1960, **38**, 144–148.
21. Hedin, A. E. *et al.*, Empirical wind model for the upper, middle and lower atmosphere. *J. Atmos. Terr. Phys*., 1996, **58**, 1421–1427.
22. Nakamura, T., Aono, T., Tsuda, T., Martimingraum, D. R. and Achmad, E., Mesospheric gravity waves over tropical convective region observed by OH airglow imaging in Indonesia, Third PSMOS International Symposium on Dynamics and Chemistry of the MLT Region, Foz do lguacu Planetary Scale Mesopause Observing System, 2002.
23. Nakamura, T., Aono, T., Tsuda, T., Admiranto, A. G., Achmad, E. and Suranto, Mesospheric gravity waves over a tropical convective region observed by OH airglow imaging in Indonesia. *Geophys. Res. Lett.*, 2003, **30**, 1882.
24. Medeiros, A. F., Buriti, R. A., Machado, E. A., Taylor, M. J., Takahashi, H., Batista, P. P. and Gobbi, D., Comparison of gravity wave activity observed by airglow imaging from two different latitudes in Brazil. *J. Atmos. Sol. Terr. Phys*., 2004, **66**, 647–655.
25. Wang, D. Y. and Tuan, T. F., Brunt Doppler ducting of small – period gravity waves. *J. Geophys. Res*., 1988, **93**, 9916–9926.
26. Swenson, G. R. and Gardner, C. S., Analytical models for the responses of the mesospheric OH* and Na to atmospheric gravity waves. *J. Geophys. Res*., 1998, **103**, 6271–6294.
27. Gavrilov, N. M., Fukao, S., Nakamura, T. and Tsuda, T., Statistical analysis of gravity waves observed with the Middle and Upper Atmospheric Radar in the middle atmosphere. 2. Waves propagated in differential directions. *J. Geophys Res*., 1997, **102**, 13433–13440.
28. Reisin, E. R. and Scheer, J., Vertical propagation of gravity waves determined from zenith observations of airglow. *Adv. Space Res*., 2001, **27**, 1743–1748.
29. Wrasse, C. M. *et al.*, Reverse ray tracing of the mesospheric gravity waves observed at 23°S (Brazil) and 7°S (Indonesia) in airglow imagers. *J. Atmos. Sol. Terr. Phys*., 2006, **68**, 163–181.

ACKNOWLEDGEMENTS. We thank the Department of Science and Technology (DST), New Delhi for funding our research in Upper Atmospheric Sciences at IIG. The night airglow observations at Kolhapur were carried out under the scientific collaboration programme (MoU) between IIG, Panvel and Shivaji University, Kolhapur.

Received 6 October 2008; revised accepted 18 December 2009